line couplers. This feature becomes more noticeable when the impedance levels deviate further away from those of the conventional coupler or the lengths differ further from quarter-wave. This is an important drawback of the present coupler, and for wider bandwidths different methods, such as the optimization technique in [3], could be used.

REFERENCES

[1] R. Levy and L. F. Lind, "Synthesis of symmetrical branch-guide directional couplers," *IEEE Trans. Microwave Theory Tech.*, vol. MTT-16, pp. 80–89, Feb. 1968.

[2] R. Levy, "Zolotarev branch-guide couplers," *IEEE Trans. Microwave Theory Tech.*, vol. MTT-21, pp. 95–99, Feb. 1973.

[3] M. Muraguchi, T. Yukitake, and Y. Naito, "Optimum design of 3-dB branch-line couplers using microstrip lines," *IEEE Trans. Microwave Theory Tech.*, vol. MTT-31, pp. 674–678, Aug. 1983.

[4] C. H. Ho, L. Fan, and K. Chang, "Broad-band uniplanar hybrid-ring and branch-line couplers," *IEEE Trans. Microwave Theory Tech.*, vol. 41, pp. 2116–2124, Dec. 1993.

[5] J. Reed and G. J. Wheeler, "A method of analysis of symmetrical four-port networks," *IRE Trans. Microwave Theory Tech.*, vol. MTT-4, pp. 246–252, Oct. 1956.

[6] T. Okoshi, T. Imai, and K. Ito, "Computer-oriented synthesis of optimum circuit pattern of 3-dB hybrid ring by the planar circuit approach," *IEEE Trans. Microwave Theory Tech.*, vol. MTT-29, pp. 195–202, Mar. 1981.

A Simple Equation for Analysis of Nonuniform Transmission Lines

Robert Nevels and Jeffrey Miller

***Abstract*—The solution to the telegrapher equations is often presented as a D'Alembert expression for the voltage in terms of the voltage at a previous time or for the current in terms of the current at a previous time. In this paper, we present a complete solution for the coupled set of transmission-line equations such that the voltage or current is in terms of both the previous time voltage and current amplitudes. The key features of these equations are: they require only the initial voltage and current amplitudes, positive- and negative-direction traveling waves do not have to be identified, they are valid on a nonuniform transmission line, and they are related to the frequency-domain $ABCD$-parameter equations and the D'Alembert expressions for coupled functions. A method is presented for evaluating this set of equations numerically and results are given for a transmission-line filter and for a transmission line with a nonuniform section.**

***Index Terms*—Distributed parameter circuits, transmission lines.**

I. INTRODUCTION

In many textbooks, e.g., [1], general real-time solutions to the transmission-line voltage and current wave equations

$$\frac{\partial^2 V}{\partial z^2} = LC\frac{\partial^2 V}{\partial t^2} \tag{1a}$$

$$\frac{\partial^2 I}{\partial z^2} = LC\frac{\partial^2 I}{\partial t^2} \tag{1b}$$

Manuscript received December 17, 1999. This work was supported by the National Science Foundation under Grant ECS-9811094 and under Grant ECS-9820644.

The authors are with the Department of Electrical Engineering, Texas A&M University, College Station, TX 77843 USA.

Publisher Item Identifier S 0018-9480(01)02433-4.

for a lossless line are given, respectively, by the D'Alembert solutions

$$V(z,t) = V^+\left(t - \frac{z}{v}\right) + V^-\left(t + \frac{z}{v}\right) \tag{2a}$$

$$I(z,t) = I^+\left(t - \frac{z}{v}\right) + I^-\left(t + \frac{z}{v}\right) \tag{2b}$$

where L and C are the transmission-line inductance and capacitance per unit length and $v = 1/\sqrt{LC}$ is the velocity of the line voltage and current waves. The interpretation of (2a) is that the voltage at a particular time and position, i.e., t and z, respectively, on a transmission line is exactly equal to the sum of the forward (V^+) and reflected (V^-) traveling voltage waves that existed at a time $t' = t - z/v$, at the respective points $z' = z \mp vt$. The expression for the current (2b) can be interpreted in the same way. Although useful, implicit in (2) are the assumptions that the transmission line is uniform and that the incident and reflected voltage and current wave functions are known.

Below, we present a simple powerful alternative set of transmission-line equations in which it is not necessary to specify the direction of travel of the initial input signal or even to distinguish the incident from the reflected waves. In addition, these equations are valid when the transmission line is nonuniform. Nonuniform transmission lines are of particular importance in modern-day microwave circuits. For example, tapered lines and concatenated lines with different characteristic impedances appear both in analog and digital circuits as impedance-matching devices and filters [2], [3].

II. ANALYSIS

The transmission-line equations

$$\frac{\partial V}{\partial z} = -L\frac{\partial I}{\partial t} \tag{3a}$$

$$\frac{\partial I}{\partial z} = -C\frac{\partial V}{\partial t} \tag{3b}$$

for a two-port lossless nonuniform transmission line can be cast in the form of a single-vector equation

$$\frac{\partial \mathbf{F}}{\partial t} = \bar{\mathbf{S}}\mathbf{F} \tag{4}$$

where the voltage–current vector F and operator matrix $\bar{\mathbf{S}}$ are defined by

$$\mathbf{F} = [\,V \quad I\,]^T \tag{5}$$

$$\bar{\mathbf{S}} = -\begin{bmatrix} 0 & \frac{1}{C}\frac{\partial}{\partial z} \\ \frac{1}{L}\frac{\partial}{\partial z} & 0 \end{bmatrix}. \tag{6}$$

In the above equations, the distributed inductance (L) and capacitance (C) are each functions of position z, as are the current (I) and voltage (V), which are also functions of time. A solution to (4) can be found by first finding the propagator matrix $\overline{\mathbf{K}}$ that satisfies [4]

$$\frac{\partial \overline{\mathbf{K}}}{\partial t} = \overline{\mathbf{S}\mathbf{K}} \tag{7}$$

with the initial condition

$$\lim_{t\to 0}\overline{\mathbf{K}} = \bar{\mathbf{I}}\delta\left(z - z'\right) \tag{8}$$

where δ is the Dirac delta function, z' is the initial position of the voltage and current at time $t = 0$, and $\bar{\mathbf{I}}$ is the identity matrix. A solution to (7), subject to (8), is

$$\bar{\mathbf{K}} = e^{\bar{\mathbf{S}}t}\delta\Big(z - z'\Big). \tag{9}$$

The matrix exponential on the right-hand side of (9) is expanded in an exponential series, each term of which is allowed to operate on a Fourier integral representation of the delta function. The terms of the series are collected, once again producing a matrix exponential that now resides inside the Fourier integral, given by

$$\bar{\mathbf{K}} = \frac{1}{2\pi}\int_{-\infty}^{\infty} e^{\bar{\mathbf{S}}t}\exp\Big[jk_z(z - z')\Big]dk_z \tag{10}$$

$$\bar{\mathbf{S}} = -\begin{bmatrix} 0 & \dfrac{jk_z}{C} \\ \dfrac{jk_z}{L} & 0 \end{bmatrix}. \tag{11}$$

The exponential $e^{\bar{\mathbf{S}}t}$ can be converted to a standard 2×2 matrix via the resolvent matrix method, which can be found in texts on state variables, e.g., [5]. The resulting propagator is

$$\bar{\mathbf{K}} = \frac{1}{2\pi}\int_{-\infty}^{\infty}\begin{bmatrix} \cos(k_z vt) & -jZ_0\sin(k_z vt) \\ \dfrac{-j\sin(k_z vt)}{Z_0} & \cos(k_z vt) \end{bmatrix} \times \exp\Big[jk_z(z - z)\Big]dk_z \tag{12}$$

where the characteristic impedance $Z_0 = \sqrt{L/C}$ and velocity v are both functions of the unprimed coordinate z. The purpose of the propagator is to transition, over the time period t, an initial voltage and current distribution $(V(z), I(z))$ into the present time voltage and current $(V(z,t), I(z,t))$. This is carried out mathematically by spatially convolving the propagator with the initial voltage and current, of which operation is expressed as

$$\begin{bmatrix} V(z,t) \\ I(z,t) \end{bmatrix} = \frac{1}{2\pi}\int_{-\infty}^{\infty}\left\{\int_{-\infty}^{\infty}\begin{bmatrix} \cos(k_z vt) & -jZ_0\sin(k_z vt) \\ \dfrac{-j\sin(k_z vt)}{Z_0} & \cos(k_z vt) \end{bmatrix} \cdot \exp\Big[jk_z(z - z)\Big]dk_z\right\}\begin{bmatrix} V(z') \\ I(z') \end{bmatrix}dz' \tag{13}$$

The propagator in (13) can be evaluated analytically yielding

$$\begin{bmatrix} V(z,t) \\ I(z,t) \end{bmatrix} = \frac{1}{2}\int_{-\infty}^{\infty}\begin{bmatrix} [\delta(z+vt)+\delta(z-vt)] & -Z_0[\delta(z+vt)-\delta(z-vt)] \\ \dfrac{-[\delta(z+vt)-\delta(z-vt)]}{Z_0} & [\delta(z+vt)+\delta(z-vt)] \end{bmatrix} \cdot \begin{bmatrix} V(z') \\ I(z') \end{bmatrix}dz' \tag{14}$$

where $z = z - z'$. Since there are delta functions in each term, (14) can also be analytically evaluated, giving the final set of equations

$$V(z,t) = \frac{\Big[V(z+tv) + V(z-tv)\Big]}{2} + \frac{Z_0\Big[I(z+tv) - I(z-tv)\Big]}{2} \tag{15a}$$

$$I(z,t) = \frac{\Big[V(z+tv) - V(z-tv)\Big]}{2Z_0} + \frac{\Big[I(z+tv) + I(z-tv)\Big]}{2}. \tag{15b}$$

An interpretation of (15) is as follows: the present time voltage, or the present time current, is found by taking sum and difference combinations of the previous time–voltage *and* the previous time–current amplitudes. The previous time voltage and current lie at the positions $z \pm t/v$, as in (2); however, the information supplied here is the *total* amplitudes at these points. That is, in contrast to (2), the positive and negative traveling voltage and current wave amplitudes do not have to be known. This provides a distinct advantage since, given only the total voltage and current distribution on the transmission line at any point in time, (15) will automatically filter out the positive and negative traveling waves and, through successive time steps, provide the complete succeeding time response of the transmission line. An alternative derivation of (15), based on the method of characteristics, has been presented in [6] and [7] for a homogeneous line.

Finally, an important observation is that the derivation of (15) was carried out assuming the inductance (L) and capacitance (C) are functions of position. These equations are, therefore, valid for nonuniform transmissions lines. In the following section, examples are given that demonstrate this property. It will also be shown that these equations are self sufficient, i.e., other than an initial voltage and current distribution and the characteristic impedance distribution, no additional information is needed to determine the time evolution of the signal.

III. Results

In the numerical method, the initial time is set to t' rather than zero, as was done in the derivation above, because its value will change as the time history of the voltage and current waves are computed. The time increment between the initial time and the present time t is chosen to be a constant τ, i.e., $\tau = t - t'$, which is related to the numerical spatial increment Δz and the velocity of light v by $\tau = \Delta z/v$. This allows us to make the replacements $t \to \tau$ and, therefore, $\tau v \to \Delta z$ in (15), resulting in

$$V(z,t) = \frac{\Big[V(z+\Delta z)+V(z-\Delta z)\Big]}{2} + \frac{Z_0\Big[I(z+\Delta z)-I(z-\Delta z)\Big]}{2} \tag{16a}$$

$$I(z,t) = \frac{\Big[V(z+\Delta z)-V(z-\Delta z)\Big]}{2Z_0} + \frac{\Big[I(z+\Delta z)+I(z-\Delta z)\Big]}{2} \tag{16b}$$

which are convenient for numerical implementation. In (16), the characteristic impedance Z_0 is evaluated at the point z, while the contributions from the previous time voltage and current are from points $z \pm \Delta z$.

Usually a transmission line is nonuniform either because the characteristic impedance or the dielectric constant of the material between the conductors changes along the line. For a position-dependent dielectric constant, the spatial increment Δz is allowed to change along the nonuniform transmission line according to $\Delta z = \tau v = \Delta l/\sqrt{\varepsilon_r(z)}$, where $\varepsilon_r(z)$ is the dielectric constant and Δl is the numerical spatial increment when $v = c$, which is the speed of light in a vacuum. However, on a typical nonuniform transmission line, the constitutive parameters remain constant, while Z_0 varies continuously or changes abruptly, as is the case at the junction of two transmission lines with different characteristic impedances. When ε_r is a constant, which is chosen for our following examples, Δz remains constant along the entire length of the line.

Fig. 1 shows a rectangular digital pulse propagating on a transmission line constructed with two sections, one having a characteristic impedance of 50 Ω and the other 75 Ω. Here, the spatial segment width Δz has been chosen to be 0.01 cm. The constitutive parameters are chosen to be that of air in both transmission-line sections, thereby

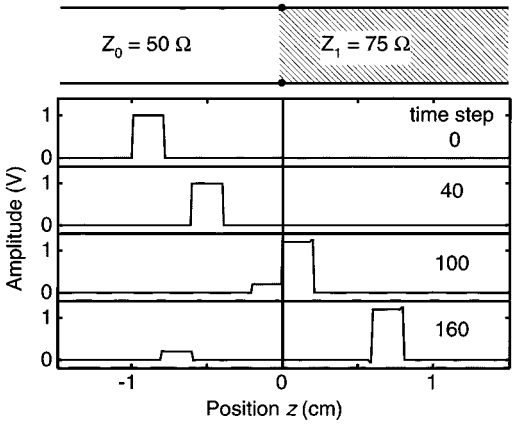

Fig. 1. Propagation of a rectangular digital pulse on two sections of transmission line with characteristic impedances $Z_0 = 50\ \Omega$ and $Z_1 = 75\ \Omega$.

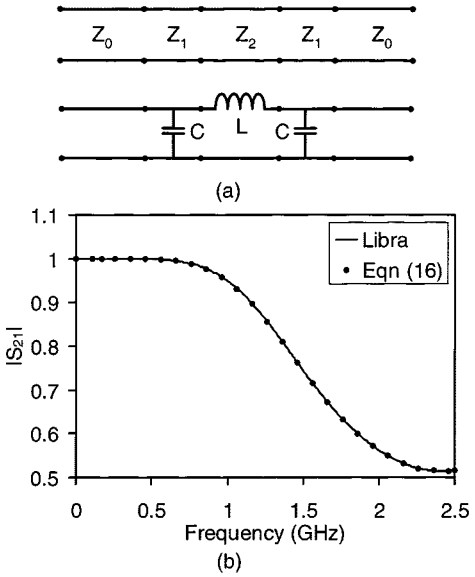

Fig. 2. (a) Transmission-line filter with its (b) frequency response [comparison of the results obtained with Libra and those based on (15)].

yielding the time increments $\tau = 0.33$ ps. The top graph shows the initial input voltage pulse, which has a width of 20 spatial increments (0.20 cm or 6.67 ps) and an amplitude of 1 V. Not pictured is an associated input current pulse with the same amplitude, but divided by the 50-Ω characteristic impedance. Each application of (16), which are computed at all segment nodes, propagates the voltage and current-one time interval τ. The remaining graphs of Fig. 1 show the evolution of the pulse after 40, 100, and 160 time steps. In the final graph, the numerically computed reflected and transmitted pulse amplitudes, i.e., 0.2 and 1.2 V respectively, were found to be accurate to five decimal places using single precision numerical arithmetic when compared to the exact analytical reflection and transmission coefficients. Both reflected and transmitted pulses exhibit ringing on the leading and trailing edges, as has been observed in laboratory measurements.

Fig. 2(a) shows as series of concatenated transmission-line sections with $Z_0 = 50\ \Omega$, $Z_1 = 30\ \Omega$, and $Z_2 = 80\ \Omega$. Since the distributed capacitance effect dominates in a transmission-line section with a low characteristic impedance and distributed inductance dominates in a high characteristic impedance section, this transmission line creates an L–C low-pass filter, as depicted in the figure. The lengths of the transmission-line sections with characteristic impedances Z_1 are 2.022 cm and the section with characteristic impedances Z_2 is 2.128-cm long.

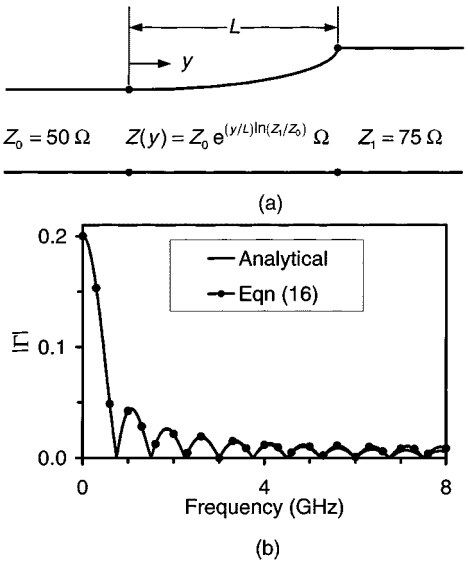

Fig. 3. (a) Nonuniform transmission-line section with its (b) reflection coefficient versus frequency [comparison of exact result with numerical calculations based on (15)].

The spatial segment has been chosen to be $\Delta z = 1 \times 10^{-4}$ cm and, as above, the inductance and capacitance in the 50-Ω line are chosen so as to produce a phase velocity equal to the speed of light in a vacuum. The time increment is, therefore, $\tau = 33 \times 10^{-4}$ ps. The time-domain response of this transmission-line configuration found using (16) with a Gaussian pulse excitation is Fourier transformed and compared to that obtained using Libra [8] computer-aided design (CAD) software. The results shown in Fig. 2(b) are indistinguishable.

Fig. 3(a) shows a nonuniform transmission-line section of length L, sandwiched between two uniform lines with characteristic impedances $Z_0 = 50\ \Omega$ and $Z_1 = 75\ \Omega$. The characteristic impedance of the nonuniform section is $Z(y) = Z_0 \exp[(y/L)\ln(Z_1/Z_0)]$. The reflection coefficient, again obtained by Fourier transformation of the time-domain result, computed using (16) with a Gaussian excitation pulse, is compared in Fig. 3(b) with the exact result [2]. A taper length $L = 0.2$ m and segment width $\Delta z = 0.01$ m allow only 20 cells in the nonuniform line region, which is sufficient for good agreement over the frequency range of 0–6 GHz. Greater accuracy can be achieved by using smaller segments.

IV. Conclusions

A time-domain solution for the coupled telegrapher's equations has been presented in this paper. Each of the two equations in this solution only requires knowledge of the previous time total voltage and current. It has been shown that, in order to determine the complete time history of a signal, it is necessary to only know an initial input voltage and current and the characteristic impedance or, equivalently, the constitutive parameters of a transmission line. This set of equations is simple to implement numerically and has been shown to give good results with two and five transmission-line sections and with a nonuniform transmission line. It has been observed that, with these equations, the transmission-line signal is not subject to numerical dispersion. A fascinating property of these equations is that positive- and negative-direction waves are automatically recognized and propagated in their respective directions given only initial voltage and current amplitudes.

A interesting observation is that (13) can be converted to frequency-domain form by replacing the time-domain voltage and current $V(z,t)$ and $I(z,t)$ by their respective frequency-domain counterparts $V(z,\omega)$ and $I(z,\omega)$. This replacement, along with a

time–harmonic initial voltage and current $Ve^{-jk_0z'}$ and $Ie^{-jk_0z'}$, and again defining $\Delta z = \tau v$, leads to

$$\begin{bmatrix} V(z) \\ I(z) \end{bmatrix} = \begin{bmatrix} \cos(k_o\Delta z) & jZ_0\sin(k_o\Delta z) \\ \dfrac{j\sin(k_o\Delta z)}{Z_0} & \cos(k_o\Delta z) \end{bmatrix} \begin{bmatrix} Ve^{-jk_oz} \\ Ie^{-jk_oz} \end{bmatrix} \quad (17)$$

The bracketed matrix term in (17) is the well-known time–harmonic two-port transmission-line $ABCD$-parameter matrix. Using this result, it can be reasoned that (15) is the time-domain equivalent to the frequency-domain $ABCD$ matrix (17).

Finally, it is observed that a traditional D'Alembert solution for the coupled system (3) can be extrapolated from (15) by removing those portions of the previous time V and I that do not contribute to the present time $V(z, t)$, $I(z, t)$ as follows:

$$V(z,t) = \frac{\left[V^-(z+tv) + V^+(z-tv)\right]}{2} + \frac{\left[Z_0^-I^-(z+tv) - Z_0^+I^+(z-tv)\right]}{2} \quad (18a)$$

$$I(z,t) = \frac{\left[V^-(z+tv)/Z_0^- - V^+(z-tv)/Z_0^+\right]}{2} + \frac{\left[I^-(z+tv) + I^+(z-tv)\right]}{2}. \quad (18b)$$

It can be easily shown that (18) reduce to (2) by making the substitutions $Z_0^\pm = \pm V^\pm/I^\pm$ in (18) and recognizing that the arguments $t \pm z/v$ and $z \pm tv$ have the same interpretation.

REFERENCES

[1] N. N. Rao, *Elements of Electromagnetic Engineering*, 5th ed. Englewood Cliffs, NJ: Prentice-Hall, 2000.

[2] R. E. Collin, *Foundations for Microwave Engineering*. New York: McGraw-Hill, 1966, sec. 5.12.

[3] P. Pramanick and P. Bhartia, "A generalized theory of tapered transmission line matching transformers and asymmetric couplers supporting non-TEM modes," *IEEE Trans. Microwave Theory Tech.*, vol. 37, pp. 1184–1190, Aug. 1989.

[4] G. Barton, *Elements of Green's Functions and Propagation*. New York: Oxford, 1989.

[5] P. M. DeRusso, R. J. Roy, and C. M. Close, *State Variables for Engineers*. New York: Wiley, 1965.

[6] P. L. E. Uslenghi, "Pulse propagation on lossy lines," in *AMEREM'96 Dig.*, Albuquerque, New Mexico, May 1996, p. 348.

[7] ——, "On the time-domain analysis of transmission lines," in *IEEE AP-S Int. Symp. Dig.*, Atlanta, GA, June 1998, p. 888.

[8] *Libra: A Software Simulator for Microwave and RF Circuits, Version 6.1*. Westlake Village, CA: HP-EEsof, 1999.

Etched-Silicon Micromachined W-Band Waveguides and Horn Antennas

Bassem A. Shenouda, L. Wilson Pearson, and James E. Harriss

***Abstract*—Micromachining of silicon is broadly proposed for the fabrication of substrates and waveguides at millimeter wavelengths. This paper presents the results of the fabrication of finned diamond-shaped waveguides and horn antennas by way of ethylene–diamene–pyrocatechol anisotropic etching of silicon. The structure is fabricated in two halves by etching V grooves in (100) silicon wafers. The etched faces of the wafers were metallized with gold. Metallic fins evaporated on a thin layer of Mylar and sandwiched between the two halves of the structure were used to improve the bandwidth of the waveguide. Measurements were taken of the dispersion curve of the waveguide with fins with different gap separations, and of the radiation patterns of the fabricated horns with different flare angles at different frequencies. Measurements showed a very good agreement with numerical calculations using the finite-element-method technique. Computed attenuation curves for the structure are provided as well.**

***Index Terms*—Horn antennas, micromachining, millimeter wave antennas.**

I. INTRODUCTION

Silicon micromachining has been used to fabricate millimeter-wave horn antennas and waveguides [1]–[3]. The flare angle of the previously reported fabricated antennas [1], [2] was limited to 70.52° by the (111) silicon crystal planes. To overcome the angle limitation, Guo [2] and Johansson and Whyborn [4] suggested a diamond-shaped horn antenna etched in silicon, and its fabrication was first reported by the authors [5]. Crowe *et al.* reported the fabrication of receivers and mixers using a similar horn structure [6], [7]. This structure can be fabricated with different horn flare angles, which is desirable from a design point-of-view. A diamond-shaped structure arises naturally through wet-etch micromachining of a (100) silicon wafer. The waveguide walls are aligned with the (111) crystal planes, and the flare of the horns is a fine-scale corrugation of triangular cross sections, all characterized by the 70.52° angle between the (111) planes. However, since the etching process is anisotropic and the etch in the (100) direction is dominant, the final shape approximates the shape of the mask, but is corrupted to a small extent by etching in directions other than the (100) direction. Optical measurements are used to determine the actual flare angle of the fabricated structure and the dimensions of the horn opening. The measured dimensions are used in the numerical calculations.

II. FABRICATION

The antenna/waveguide assemblies depicted in Fig. 1(a) were formed by etching 3-mm-thick (100) silicon wafers using ethylene–diamene–pyrocatechol (EDP) etchant solution indicated by Wu *et al.* [8]. The wafer was masked with a pattern consisting of three pairs of waveguide/horn structures to fabricate three waveguide/horn assemblies with different horn-flare angles. The masked wafer was etched with agitation in the EDP solution at a temperature of 110 °C

Manuscript received December 15, 1999; revised May 12, 2000. This work was supported by the U.S. Federal Aviation Administration under Grant 93-G-047.

The authors are with the Holcombe Department of Electrical and Computer Engineering, Clemson University, Clemson, SC 29634-0915 USA (e-mail: bshenou@ces.clemson.edu; pearson@ces.clemson.edu; james.harriss@ces.clemson.edu).

Publisher Item Identifier S 0018-9480(01)02443-7.